J. Astrophys. Astr. (1989) **10**, 367–380

Periodic Orbits in Three-Dimensional Planetary Systems

S. Ichtiaroglou, K. Katopodis, Michalodimitrakis *Department of Theoretical Mechanics, University of Thessaloniki, 54006, Greece*

Received 1989 March 14; accepted 1989 July 14

Abstract. Three-dimensional planetary systems are studied, using the model of the restricted three-body problem for μ = .001. Families of three-dimensional periodic orbits of relatively low multiplicity are numerically computed at the resonances 3/1, 5/3, 3/5 and 1/3 and their stability is determined. The three-dimensional orbits are found by continuation to the third dimension of the vertical critical orbits of the corresponding planar problem.

Key words: celestial mechanics—families of periodic orbits—stability

1. Introduction

Most of the work on planetary systems refers to the case of planar motion. In this paper we study the case of three-dimensional (3D) motion.

A wellknown way of finding 3D-periodic orbits is to find planar orbits which are critical with respect to perturbations perpendicular to the plane of motion (vertical perturbations). These orbits can be used as starting points for the computation of families of 3D-periodic orbits (Henon 1973). We use the model of the restricted circular 3-body problem and we choose the value of μ equal to 0.001 in order for our results to apply to the case of an asteroid subjected to the gravitational attraction of the Sun and Jupiter. In Section 2 we summarize the known results on the case of planar motion.

2. Simple periodic orbits of the planar planetary problem and their stability

We consider two point masses P_2 and P_3 (planets) with masses $m_2 \neq 0$, $m_3=0$ respectively, revolving around a central point mass P_1 (Sun) with much larger mass m_1. The orbit of P_2 is circular with P_1 at its centre. The parameter μ is defined by $\mu = m_2 /m_1 + m_2$.

We define a rotating frame of reference 0xyz whose origin is the centre of mass of P_1, P_2 and its x-axis the line P_1P_2 (with the positive direction from P_1 to P_2). In our calculations the following normalization is used

$$G = 1, \qquad m_1 + m_2 = 1, \qquad \omega = 1$$

where G is the gravitational constant and ω_0 is the angular velocity of the rotating frame.

It can be proved (Birkhoff 1927; Arenstorf 1963; Guillaume 1969; Schmidt 1972) that in the rotating frame there exist families of periodic orbits, symmetric with respect to the x-axis, which can be generated by continuation with respect to μ of the periodic orbits of the corresponding degenerate ($\mu = 0$) problem. A numerical study of the above continuation is included in Colombo, Franklin & Munford (1968), Broucke (1968), Hadjidemetriou & Ichtiaroglou (1984).

A periodic orbit, of period T and multiplicity m, (*i.e.* the number of crossings with the $y = 0$ plane during a semiperiod), which is symmetric with respect to the rotating x-axis starts perpendicularly from the x-axis ($y_0 = \dot{x}_0 = 0$) and again crosses perpendicularly the x-axis. Consequently it can be represented by a point in the $x\dot{y}$ plane. A monoparametric family of such orbits is represented by a smooth curve in the $x\dot{y}$ plane known as the "characteristic curve" of the family. A periodic orbit of P_3 is called direct (retrograde) if P_3 revolves around P_1 in the same (opposite) direction as that of P_2 (in the inertial frame).

For $\mu = 0$ there exist the following families of simple ($m = 1$) periodic orbits of P_3 in the rotating frame:

(a) Two families of circular Keplerian orbits, the family D of direct orbits and the family R of retrograde orbits. (The family D consists of two branches corresponding to orbits inside and outside, respectively, of the orbit of P_2).

(b) An infinite number of families E_i of elliptic Keplerian orbits which bifurcate from the orbits of the family D at the resonances $n/(n+1)$ and $(n+1)/n$, ($n = 1, 2, \ldots$).

The characteristic curves of the above families are represented by broken lines in Fig. 1.

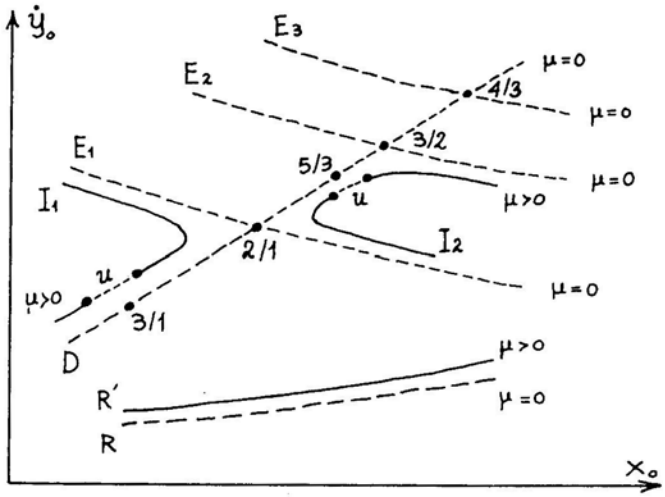

Figure 1. The families of simple planar periodic orbits of the degenerate ($\mu = 0$) and the perturbed ($\mu > 0$) planetary problem (shown schematically). R = family of retrograde circular orbits, D = family of direct circular orbits inside the orbit of P_2, R' = continuation of R for $\mu > 0$, I_1, I_2, . . . = continuation of D for $\mu > 0$, E_1, E_2, . . . = families of elliptic orbits bifurcating from the direct circular orbits at the $(n+1)/n$ ($n = 1, 2, \ldots$) resonances. The instability strips of l_i, near the resonances $(n+1)/n$ are represented by dashed lines (u).

For $\mu>0$ all orbits of the family R are continued forming a nearby family R' of nearly circular retrograde orbits. On the contrary, the continuation fails at the resonant orbits $n/(n+1)$, $(n+1)/n$ ($n = 1, 2, \ldots$) of family D and each of the resulting families I_i (for $\mu > 0$) consists of a part with nearly circular orbits while the remaining parts consist of resonant nearly elliptic orbits. The characteristic curves of the families I_i are represented by solid lines in Fig. 1.

All periodic orbits for $\mu = 0$ are evidently stable. It can be proved (Hadjidemetriou 1982) that the circular direct and retrograde degenerate orbits are strongly stable, in the sense that there exist no Hamiltonian perturbation which generates instability, with as only exception the orbits at the resonances $(2n+1)/(2n-1)$, $(2n-1)/(2n+1)$ ($n = 1,2, \ldots$) of family D where a Hamiltonian perturbation always exists which generates instability. Instability can always be generated for all elliptic orbits of the families E_i.

According to numerical computations (Hadjidemetriou & Ichtiaroglou 1984) the increase of μ from the zero value is a destabilizing perturbation which (a) creates in each of the families I_i a small strip of unstable almost circular direct orbits at the resonances $n/(n+1)$, $(n+1)/n$ (see dotted parts of I_i in fig. 1), and (b) generates instability in some elliptic branches of I_i; but not in all of them.

The above remarks refer to planar stability. As far as vertical stability is concerned, it can be proved that vertical instability can develop in the same resonant orbits as for planar stability. According to numerical computations (μ=0.001), when vertical instability develops the vertically unstable region is within the above-mentioned planar instability strips of the circular branches of I_i. Also, all elliptic branches of I_i are vertically stable.

3. Vertical bifurcations in the planar degenerate problem

3.1 *Vertical Critical Orbits*

Let $\Delta(T)$ be the monodromy matrix of the variational equations for the vertical perturbations of a plane orbit with period T (in the rotating frame). The vertical stability index (Hénon 1973) is equal to

$$a_v = \tfrac{1}{2} \text{ trace } \Delta(T). \tag{1}$$

A planar orbit Γ is vertically stable (unstable) if $|a_v| < 1$ ($|a_v| > 1$) and vertical critical if $|a_v| = 1$. If $a_v = 1$ the family of 3D-orbits which bifurcates from Γ has the same multiplicity as that of Γ while if $a_v = -1$ its multiplicity is twice that of Γ If $|a_v| < 1$ and

$$a_v = \cos\left(2\pi\frac{n_1}{n_2}\right) \tag{2}$$

where n_1, n_2 are integers and $n_1 < n_2$, the multiplicity of 3D-orbits is $n_2 m$ (where m is the multiplicity of Γ).

Since the structure of phase space is determined primarily by the low-order periodic orbits we confine ourselves to the study of "simple" ($m = 1$) and "double" ($m = 2$)

bifurcating 3D-orbits only and, consequently, in vertical critical orbits only (a_v= 1 for m = 1 and a_v = – 1 for m = 2).

For μ = 0 the equations of motion are (Szebehely 1967)

$$\ddot{x}-2\dot{y}-x=-xr^{-3}$$
$$\ddot{y}+2\dot{x}-y=-yr^{-3}$$
$$\ddot{z}=-zr^{-3}$$

where $r^2 = x^2 + y^2 + z^2$.

Let $z(t) = \xi_1(t)$, $\dot{z}(t) = \xi_2(t)$ be vertical perturbations to a circular orbit of radius R and period T (in the rotating frame). The corresponding variational equations are

$$\dot{\xi}_1=\xi_2$$
$$\dot{\xi}_2=-\omega^2\xi_1 \tag{3}$$

Where

$$\omega^2=R^{-3}. \tag{4}$$

The monodromy matrix of (3) is

$$\Delta(T)=\begin{pmatrix}\cos\omega T & \omega^{-1}\sin\omega T\\ -\omega\sin\omega T & \cos\omega T\end{pmatrix}$$

and, consequently, the vertical stability index is equal to

$$a_v = \tfrac{1}{2} \text{ trace } \Delta(T) = \cos\omega T. \tag{5}$$

The relative period T of a retrograde circular orbit is equal to $T_R = 2\pi/(\omega + 1)$ and for a direct orbit is equal to $T_D = 2\pi/|\omega - 1|$. Consequently we have

$$(a_v)_R=\cos 2\pi\frac{\omega}{\omega+1}$$

for the retrograde orbits and

$$(a_v)_D=\cos 2\pi\frac{1}{|\omega^{-1}-1|}$$

for the direct orbits.

Since $|(a_v)_R| < 1$, all retrograde circular orbits are vertically stable and therefore of no interest in the search for 3D-bifurcations with multiplicities $m \leqslant 2$. On the other hand, for suitable values of ω,$(a_v)_D$ can become equal to ± 1.Consequently, vertical critical orbits exist in the family D of direct circular orbits.

The values of the angular velocity ω of these vertical critical orbits are given in Table 1. Since $\omega^2 = R^{-3}$, $\omega > 1$ corresponds to internal orbits (R < l). From Table 1 we note that (a) the external resonant orbits with ω = 1/3, 3/5 and the internal orbits with ω = 3/1, 5/3 have a_v= –1 and consequently the bifurcating 3D-degenerate orbits are double, and (b) simple 3D-bifurcations (a_v = 1) take place at the resonances (n + 1)/n, n/(n + 1), (n = 1,2, . . .) . These latter bifurcations are of no interest here because the continuation to μ > 0 fails in this case. On the contrary, the continuation is possible if a_v = –1.

Table 1. The angular velocity ω of the vertical critical direct circular orbits ($n = 1, 2, \ldots$).

	$\omega > 1$	$(R < 1)$	$\omega = \frac{n+1}{n}$
$a_v = 1$			
	$\omega < 1$	$(R > 1)$	$\omega = \frac{n}{n+1}$
	$\omega > 1$	$(R < 1)$	$\omega = \frac{2n+1}{2n-1}$
$a_v = -1$			
	$\omega < 1$	$(R > 1)$	$\omega = \frac{2n-1}{2n+1}$

3.2 *Families of 3D-Orbits of the Degenerate Problem*

Let $0XYZ$ be an inertial frame whose Z-axis coincides with the Z-axis of the rotating frame $0xyz$. Let

$$\begin{aligned} X &= R\cos\omega t \\ Y &= R\cos\omega t.\ \cos i \\ Z &= R\cos\omega t \cdot \sin i \end{aligned} \tag{6}$$

be the equations of a circular motion of P_3 with respect to $0XYZ$, where i is the inclination of the orbit relative to the XY plane. Equations (6) in the rotating frame take the form

$$\begin{aligned} x &= R\cos\omega t \cdot \cos t + R\cos i \cdot \sin\omega t \cdot \sin t \\ y &= -R\cos\omega t \cdot \sin t + R\cos i \cdot \sin\omega t \cdot \cos t \\ z &= R\sin i \cdot \sin\omega t. \end{aligned} \tag{7}$$

The orbit is periodic in the rotating frame if ω is rational and its multiplicity m depends on ω. If $\omega = n_1/n_2$ where n_1, n_2 are relative prime integers, then the multiplicity is equal to $m = |n_1 - n_2|$.

From (7) it follows that the motion starts ($t = 0$) perpendicular to the x-axis with initial conditions

$$\begin{aligned} x_0 &= R, \quad y_0 = 0, & z_0 &= 0, \\ \dot{x}_0 &= 0, \quad \dot{y}_0 = R\omega\cos i - R, & \dot{z}_0 &= R\omega\sin i. \end{aligned} \tag{8}$$

Such a motion is symmetric with respect to the x-axis. In the $\dot{y}_0\,\dot{z}_0$ plane, Equations (8) define a monoparametric family of 3D-periodic orbits which in the inertial frame are circular with the same radius R and variable inclination.

From (8) we find that the characteristic curve of this family is given by

$$\dot{y}_0 = \pm(R^{-1} - \dot{z}_0^2)^{\frac{1}{2}} - R \tag{9}$$

where the plus sign corresponds to direct (in the inertial frame) orbits and the minus

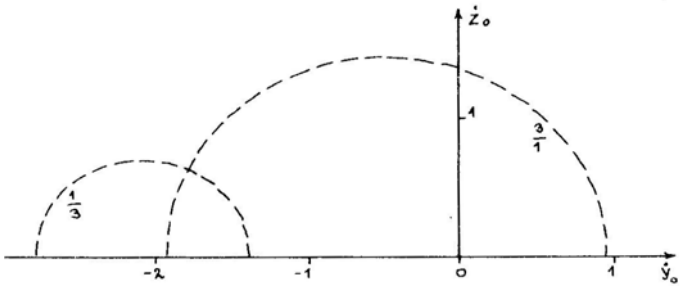

Figure 2. Characteristic curves of families of circular 3D-periodic orbits of the degenerate problem for the cases ω = 3/1 and ω= 1/3.

sign to retrograde orbits. The characteristic curves (9) are circles of radius $R^{-1/2}$ centred at (– R, 0) .See for example Fig. 2 for the cases ω = 3/1 and ω= 1/3.

As we have said before, we are interested here only in the double orbits which bifurcate from direct circular vertical critical orbits with a_v = –1, *i.e.* with ω = (2n + 1)/(2n – 1), or ω = (2n – 1)/ (2n + 1), (n = 1, 2, . . .). In these cases family (9) starts ($\dot{z}$ = 0) with a direct circular vertical critical orbits and continues ($\dot{z} \neq 0$) with double orbits which a direct (in the sense that the projected motion on the inertial the inertial *XY* plane is direct). The multiplicity of the 3D-orbits does not necessarily remain the same as we proceed along the family. At the maximum $\dot{z}_0$, where the inclination assumes its maximum value π/2, the orbits switch to retrograde and the family terminates ($\dot{z}$ = 0) with a retrograde circular orbit with $|a_v| < 1$ since all retrograde circular orbits are vertically stable.

The value of a_v of the termination orbit can be found as follows. The relative period of a retrograde orbit is $T_R = 2\pi/(1+\omega)$. Then, in the case $\omega = (2n + 1)/(2n - 1)$ we have

$$a_v = \cos\omega T_R = \cos 2\pi \frac{\omega}{1+\omega} = \cos 2\pi \frac{(2n+1)}{4n},$$

while in the case $\omega = (2n-1)/(2n+1)$ we have

$$a_v = \cos 2\pi \frac{(2n-1)}{4n}.$$

In both cases, the multiplicity of the retrograde orbit is 4n and a_v becomes equal to 1 if this orbit is considered as described 4n times (*i.e.* if its period is considered equal to $T'_R = 4nT_R$).

The diagram of the relative period T versus the radius R for the planar circular orbits of the degenerate problem is given in Fig. 3. The planar orbits are connected through 3D-families (represented by vertical dashed lines) for the cases ω = 3/1, 5/3, 3/5, 1/3.

4. Families of 3D-periodic orbits of the perturbed problem ($\mu > 0$)

The 3D-families of the perturbed problem can be viewed as resulting from a continuation to the third dimension of the vertical critical orbits of the perturbed

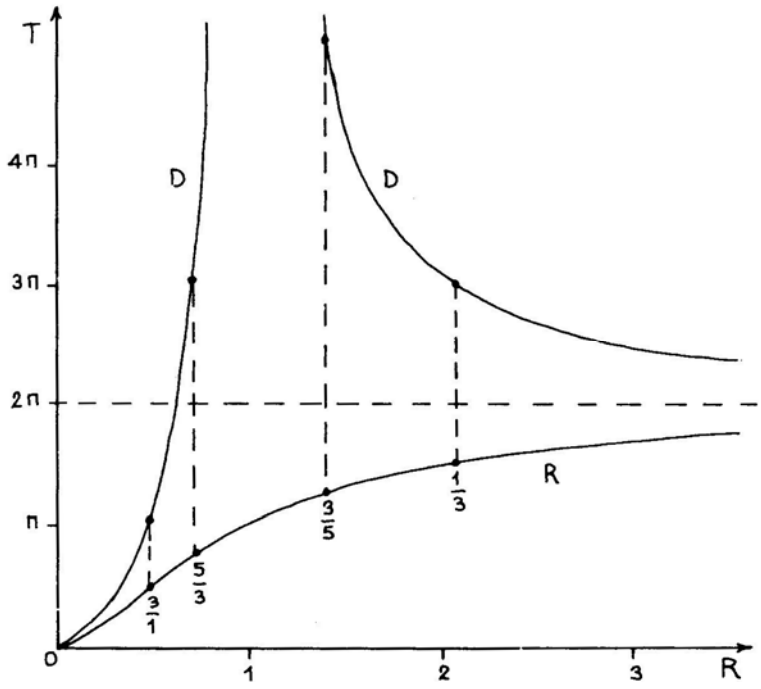

Figure 3. Relative period T versus the radius R for the families of direct (D) and retrograde (R) planar periodic orbits of the degenerate problem.

planar problem or from a continuation with respect to μ of the 3D-families of the corresponding degenerate 3D-problem.

Following the first point of view, we seek vertical critical orbits for $\mu > 0$ (here $\mu = 0.001$). The existing numerical results showed (Section 2) that the continuation with respect to μ in the neighbourhood of the resonant direct circular orbits with $\omega = (2n + 1)/(2n - 1)$ or $\omega = (2n - 1)/(2n + 1)$,($n$ = l, 2, . . .) generates on each family μ = const., a strip of vertical instability whose width increases with μ. The boundaries of these strips correspond to vertical critical orbits wiih $a_v = -1$ which can be considered as continuation of the corresponding vertical critical resonant circular orbit for $\mu = 0$ (Fig. 4). These orbits can be used as starting points for the computation of 3D-families for $\mu > 0$. In our case we choose the values $\mu = 0.001$ and ω = 3/1, 5/3, 1/3, 3/5.

Let us now follow the second point of view. To be specific, we consider the 3D-degenerate family (9) which starts ($\dot{z}_0 = 0$) from the vertical critical ($a_v = -1$) direct internal ($R < 1$) circular orbit Γ at the ω = 3/1 resonance and terminates ($\dot{z}_0 = 0$) at the vertical stable retrograde internal circular orbit Γ_2, with $a_v = \cos 2\pi(1/4)$ and multiplicity $m = 4$. Let Γ'_1 and Γ''_1 be the vertical critical orbits ($a_v = -1$) which are the continuation of Γ_1 with respect to μ Γ'_2 the corresponding continuation of Γ_2.

As can be seen from Fig. 5, the continuation with respect to μ of the 3D-degenerate family which joins Γ_1 with Γ_2, leads to two 3D-families (with $\mu > 0$) which start from Γ'_1 and Γ''_1, respectively and terminate at the same orbit Γ'_2. These two families can be considered also as continuations of Γ_2 with respect to the positive ($x > 0$) or negative ($x > 0$) intersection of Γ_2 with the x-axis.

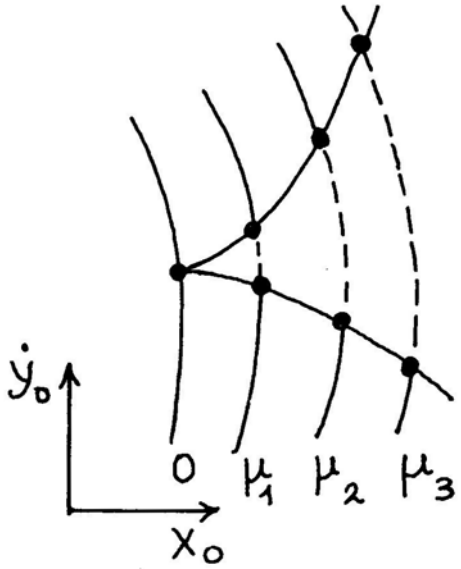

Figure 4. The instability strips around resonance $\omega = (2n + 1)/(2n - 1)$ are shown schematically on the families of planar periodic orbit for the values $\mu_1, <\mu_2<\mu_3$ of μ.

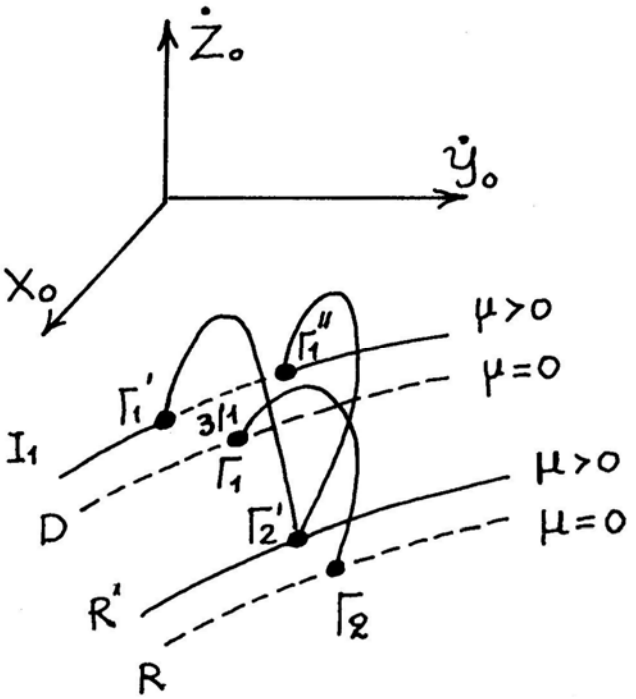

Figure 5. 3D-families bifurcating from the vertical critical direct orbits Γ_1, Γ'_1, Γ'' at the 3/1 resonance (shown schematically). The orbits Γ'_1 and are continuations of Γ_1 with respect to μ. The 3D-families emanating from Γ'_1 and Γ''_1 terminate at the vertically stable retrograde orbit Γ'_2 which is the continuation of the vertically stable retrograde orbit Γ_2. The 3D-family from Γ_1 terminates at Γ_2.

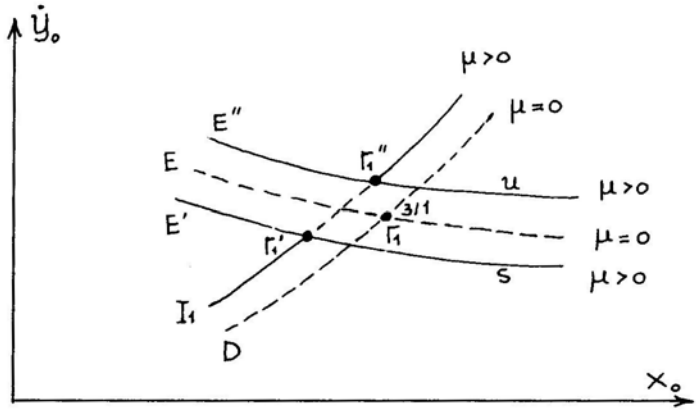

Figure 6. 2D-families bifurcating from the planar critical direct orbits Γ_1, Γ'_1, Γ''_1 at the 3/1 resonance (shown schematically). *E*, *E′*, *E″* are families of double elliptic orbits, *E′* is stable while *E″* is unstable. Γ_1, Γ'_1 is the instability strip of I_1.

An analogous situation is known to exist (Hadjidemetriou & Ichtiaroglou 1984), in the case of planar bifurcations. This situation is summarized in Fig. 6, where Γ'_1, and Γ''_1 are planar critical orbits at the ends of the plane instability strip Γ'_1,Γ'' and the bifurcating planar families *E*, *E′*, *E″* consist of double elliptic orbits (*E′* is stable while *E″* is unstable). Recall that simple elliptic orbits occur at the resonances $(n + 1)/(n - 1)$ but not $(n + 1)/n$.

5. Numerical results

We computed eight 3D-families for $\mu = 0.001$, which emanate from the vertical critical orbits of the vertical instability strips around the resonances $\omega = 3/1, 5/3$ for $R < 1$ and $\omega = 1/3, 3/5$ for $R > 1$. We also computed their stability parameters Δ, b_1, b_2 (Hadjidemetriou 1975).

A 2D-periodic orbit is linearly stable when all the roots of the characteristic equation

$$\lambda^4 + \alpha\lambda^3 + \beta\lambda^2 + \alpha\lambda + 1 = (\lambda^2 + b_1\lambda + 1)(\lambda^2 + b_2\lambda + 1) = 0$$

of the corresponding monodromy matrix *A* have modulus equal to unity. The coefficients α, β, b_1, b_2 expressed in terms of the elements of *A* are given by $\alpha = -$ trace(*A*),

$$\beta = \begin{vmatrix} \alpha_{11} & \alpha_{12} \\ \alpha_{21} & \alpha_{22} \end{vmatrix} + \begin{vmatrix} \alpha_{11} & \alpha_{13} \\ \alpha_{31} & \alpha_{33} \end{vmatrix} + \begin{vmatrix} \alpha_{11} & \alpha_{14} \\ \alpha_{41} & \alpha_{44} \end{vmatrix} + \begin{vmatrix} \alpha_{22} & \alpha_{23} \\ \alpha_{32} & \alpha_{33} \end{vmatrix} + \begin{vmatrix} \alpha_{22} & \alpha_{24} \\ \alpha_{42} & \alpha_{44} \end{vmatrix} + \begin{vmatrix} \alpha_{33} & \alpha_{34} \\ \alpha_{43} & \alpha_{44} \end{vmatrix},$$

$$b_1 = \tfrac{1}{2}(\alpha + \sqrt{\Delta}),\ b_2 = \tfrac{1}{2}(\alpha - \sqrt{\Delta})$$

where $\Delta = \alpha^2 - 4(\beta - 2)$.

The orbit is stable when

$$\Delta > 0, \quad |b_1| < 2, \quad |b_2| < 2.$$

Broucke (1969) found that there exist seven stability regions in the $\alpha - \beta$ plane, only one of which corresponds to stable motion.

Some representative results are shown in Tables 2–9 where the initial conditions $\dot{z}_0$, x_0, y_0, the semiperiod $T/2$, the multiplicity m, the stability indices b_1, b_2, the sign of Δ, the stability region and finally the stability of the periodic orbits are given. Stable orbits are characterized by the letter 's' and unstable orbits by 'u'. Orbits whose stability is characterized by the letter 'c' lie, within the accuracy of our computations, on the borderline between the stability regions 1 and 7. For such orbits b_1 and b_2 are very close to the value 2 and the value of Δ is very close to zero. The planar orbits ($\dot{z}_0 = 0$) are characterized by their planar stability character.

The eight families which are given in the Tables are named A_{mn} or B_{mn} where the letter A or B refers to the initial point ($x_0 < 0$ or $x_0 > 0$ respectively), while the indices m, n refer to the type of resonance, *i.e.* $\omega = m/n$. The last orbits of each pair of families A_{mn}, B_{mn} are the same.

Table 2. Family A_{31}.

$\dot{z}_0$	x_0	$\dot{y}_0$	$T/2$	m	b_1	b_2	sign Δ	Region	Stability
.0	−.481041	−.963187	1.5698	1					u
.2	−.481074	−.949148	3.1396	2	11.408	2.001	+	6	u
.4	−.481161	−.906221	3.1399	2	10.598	1.760	+	6	u
.8	−.481398	−.719756	3.1405	2			−		u
1.2	−.481583	−.318853	3.1412	2	−1.307	−2.492	+	7	u
1.4	−.481595	.825784	3.1418	4	−1.993	−2.002	+	7	u
1.2	−.481597	1.280071	3.1422	4	−1.995	−2.002	+	7	u
.8	−.481670	1.680080	3.1425	4	−2.000	−2.000	+	1–7	c
.4	−.481760	1.865634	3.1428	4	−2.000	−2.000	+	1–7	c
.2	−.481790	1.908250	3.1429	4	−2.000	−2.000	+	1–7	c
.0	−.481801	1.922174	0.7858	1					s

Table 3. Family B_{31}.

$\dot{z}_0$	x_0	$\dot{y}_0$	$T/2$	m	b_1	b_2	sign Δ	Region	Stability
.0	.479319	.962528	1.5706	1					u
.2	.479320	.948595	3.1411	2	−2.000	−2.001	+	7	u
.4	.479321	.905958	3.1411	2	−2.000	−2.003	+	7	u
.8	.479333	.720340	3.1411	2	−2.000	−2.011	+	7	u
1.2	.479380	.320336	3.1412	2	−2.000	−2.023	+	7	u
1.4	.479586	−.826108	3.1416	4	−1.025	−10.515	+	7	u
1.2	.479662	−1.279920	3.1418	4	10.589	2.027	+	6	u
.8	.479691	−1.680156	3.1423	4	23.563	2.187	+	4	u
.4	.479666	−1.865975	3.1427	4	31.102	2.013	+	4	u
.2	.479652	−1.908676	3.1428	4	32.941	1.973	+	6	u
.0	.479647	−1.922631	0.7857	1					s

The last orbits of A_{31} and B_{31} are the same.

Table 4. Family A_{53}.

$\dot{z}_0$	x_0	$\dot{y}_0$	$T/2$	m	b_1	b_2	sign Δ	Region	Stability
.0	−.718653	−.456232	4.6999	1					u
.2	−.717907	−.441304	9.4053	2	.637	−2.515	+	7	u
.4	−.716649	−.392144	9.4136	2	1.903	−3.196	+	7	u
.6	−.715655	−.301054	9.4188	2	1.843	−3.788	+	7	u
.8	−.714906	−.154951	9.4216	2	1.780	−4.471	+	7	u
1.1	−.712487	1.152084	9.4260	8	−1.871	−2.004	+	7	u
1.0	−.712223	1.347685	9.4266	8	−1.902	−2.003	+	7	u
.8	−.711970	1.586217	9.4282	8	−1.954	−2.002	+	7	u
.6	−.711995	1.733786	9.4304	8	−1.987	−2.002	+	7	u
.2	−.713127	1.879403	9.4383	8	−2.000	−2.000	+	1–7	c
.0	−.713627	1.896227	1.1801	1					s

Tables 5. Family B_{53}.

$\dot{z}_0$	x_0	$\dot{y}_0$	$T/2$	m	b_2	b_2	sign Δ	Region	Stability
.0	.712522	.470716	4.7082	1					u
.2	.712295	.454148	9.4169	2	−2.016	−2.185	+	5	u
.6	.711077	.310490	9.4199	2	−2.008	−2.926	+	5	u
.8	.710496	.164241	9.4214	2	−2.004	−2.878	+	5	u
1.1	.710262	−1.154799	9.4255	8	23.860	3.570	+	4	u
1.0	.710374	−1.348867	9.4262	8	30.934	3.059	+	4	u
.8	.710486	−1.586787	9.4278	8	39.864	2.544	+	4	u
.4	.710549	−1.827966	9.4337	8	48.769	2.155	+	4	u
.2	.710681	−1.880541	9.4383	8	50.656	2.085	+	4	u
.0	.710821	−1.897531	1.1801	1					s

The last orbits of B_{53} and A_{53} are the same.

Table 6. Family A_{35}.

$\dot{z}_0$	x_0	$\dot{y}_0$	$T/2$	m	b_1	b_2	sign Δ	Region	Stability
.0	−1.416162	.578480	7.8441	1					u
.2	−1.412653	.597352	15.6952	2	−1.661	−2.017	+	7	u
.4	−1.408656	.668254	15.7024	2	−1.389	−2.005	+	7	u
.6	−1.406668	.815074	15.7057	2	−1.373	−2.002	+	7	u
.8	−1.407194	1.671639	15.7088	8	−1.760	−2.000	+	1–7	c
.6	−1.408014	1.999227	15.7105	8	−1.921	−2.000	+	1–7	c
.4	−1.408239	2.149660	15.7131	8	−1.987	−2.000	+	1–7	c
.2	−1.408174	2.226902	15.7177	8	−1.999	−2.000	+	1–7	c
.0	−1.408054	2.251174	1.9652	1					s

Let us summarize the most important results of our numerical study.

1. Retrograde circular orbits are more stable than the direct ones with respect to perturbations perpendicular to the plane of motion.

2. Simple or double 3D-bifurcations do not exist for the elliptic branches of the planar families (with $\mu > 0$).

Table 7. Family B_{35}.

$\dot{z}_0$	x_0	$\dot{y}_0$	$T/2$	m	b_1	b_2	sign Δ	Region	Stability
.0	1.410079	−.570743	7.8507	1					u
.2	1.410197	−.594822	15.7021	2			−		u
.4	1.410337	−.671608	15.7038	2			−		u
.6	1.410125	−.821120	15.7055	2			−		u
.8	1.406784	−1.673572	15.7084	8	9.890	2.405	+	4	u
.6	1.405718	−1.999322	15.7102	8	10.185	2.167	+	4	u
.4	1.405898	−2.149213	15.7129	8	10.384	2.056	+	4	u
.2	1.407207	−2.226915	15.7176	8	10.470	2.001	+	4	u
.0	1.408530	−2.251817	1.9652	1					s

The last orbits of B_{35} and A_{35} are the same.

Table 8. Family A_{13}.

$\dot{z}_0$	x_0	$\dot{y}_0$	$T/2$	m	b_1	b_2	sign Δ	Region	Stability
.0	−2.080660	1.387351	4.7117	1					u
.2	−2.080501	1.416660	9.4236	2	−1.994	−2.000	+	1–7	c
.4	−2.080368	1.514133	9.4241	2	−1.982	−2.000	+	1–7	c
.6	−2.080221	1.732938	9.4245	2	−1.976	−2.002	+	7	u
.65	−2.080178	1.839094	9.4246	2	−1.976	−2.001	+	7	u
.65	−2.080135	2.321455	9.4250	4	−1.985	−2.000	+	1–7	c
.6	−2.080178	2.427677	9.4251	4	−1.988	−2.000	+	1–7	c
.5	−2.080288	2.560673	9.4252	4	−1.993	−2.000	+	1–7	c
.2	−2.080648	2.744532	9.4256	4	−1.999	−2.000	+	1–7	c
.0	−2.080749	2.774094	2.3564	1					s

Table 9. Family B_{13}.

$\dot{z}_0$	x_0	$\dot{y}_0$	$T/2$	m	b_1	b_2	sign Δ	Region	Stability
.0	2.080675	−1.387520	4.7122	1					u
.2	2.080634	−1.416936	9.4244	2	2.046	−.819	+	6	u
.4	2.080515	−1.514319	9.4245	2	2.029	−.861	+	6	u
.6	2.080345	−1.732928	9.4246	2	2.009	−.939	+	6	u
.6	2.080331	−2.427857	9.4249	4	1.919	.198	+	1	s
.4	2.080520	−2.646878	9.4252	4	1.971	.104	+	1	s
.2	2.080716	−2.744616	9.4255	4	1.995	.067	+	1	s
.0	2.080811	−2.774185	2.3564	1					s

The last orbits of B_{13} and A_{13} are the same.

3. Simple 3D-bifurcations do not exist for the circular branch of the plane families (with $\mu > 0$).

4. 3D-bifurcations exist for the family D of direct circular orbits of the degenerate problem at the resonances $n/(n+1)$, $(n+1)/n$ (n = 1, 2, . . .) but they cannot be continued for $\mu > 0$.

5. Double 3D-bifurcations exist, both for $\mu = 0$ and $\mu > 0$, from the above family D at the resonances $(2n+ 1)/(2n - 1)$ and $(2n - 1)/(2n + 1)(n = 1, 2, \ldots)$. For each resonance, a pair of vertical critical orbits exists (for $\mu > 0$) at the ends of a small strip of vertical instability. The corresponding pair of double 3D-bifurcating families consists of direct (in the inertial frame) orbits up to the maximum $\dot{z}_0$. Then the orbits become retrograde and the two families terminate ($\dot{z}_0 = 0$) at the same vertically stable orbit of family R.

6. The computed 3D-orbits are, in general, unstable. Stable orbits were found at the resonance 1/3 only. The retrograde branch of family B_{13} is the only stable branch. There are no stable 3D-bifurcations (of multiplicity $m \leqslant 2$) inside P_2.

7. There is no apparent connection between inclination and instability. We found stable orbits of high inclination while most of the low-inclination orbits are unstable. Therefore low inclination is not necessarily connected with stability nor is high inclination connected with instability.

6. Application to specific dynamical systems

As mentioned in the introduction, we selected the value $\mu = 0.001$ so that our results would apply to the case of an asteroid subjected to the gravitational attraction of Sun and Jupiter (P_2). Let us consider, for example, the Kirkwood gap at the 3/1 resonance. As is known (Hadjidemetriou & Ichtiaroglou 1984) although circular asteroid orbits do not exist there, double elliptic asteroid orbits exist, like those of Alinda (887), Hestia (46) and Maria (170). These orbits belong to the stable member of the pair of the 2D-bifurcating families at the 3/1 resonance (Fig. 6). If the same was true for the 3D-bifurcating families at the 3/1 resonance, then we would have found stable 3D-asteroid orbits. However, our results show that all computed 3D-asteroid orbits (families A_{31}, $B_{31,}$ A_{53}, B_{53}) are unstable. This is not surprising because in all computed 3D-families of the circular restricted problem, stable orbits are rare (for example, Michalodimitrakis 1979; Zagouras & Markellos 1977). The inclinations of most asteroids are relatively small so that their motion can be considered as resulting from a vertical perturbation to vertically stable planar orbits.

The fact that retrograde orbits are more stable than direct ones is not restricted to the case of vertical stability but also to that of planar stability. The same is true for other dynamical systems, for example in galactic dynamics (Contopoulos & Papayannopoulos 1980). The reason for this difference between direct and retrograde orbits in the case of planetary systems is explained by Hadjidemetriou (1979, 1985) who investigated using the theory of Krein (1950) and Gelfand Lindskii (1955) the mechanisms by which instability develops. Hadjidemetriou proves that in the retrograde case all planetary systems are stable (for small perturbations) while in the direct case instabilities are generated at some "dangerous" resonances. We believe that, basically, the same mechanism is responsible for these stability differences in other dynamical systems.

Small strips of vertical instability which give rise to 3D-bifurcations near some resonant planar orbits exist not only in planetary systems but in other dynamical systems also, for example, the Binney strips of vertical instability at the vertical resonances for the flow (caused by vertical perturbations) of material out of the galactic plane (Binney 1978, 1981). Also, 3D-families linking retrograde with direct planar

orbits exist not only in planetary systems but in galactic dynamics as well (Mulder & Hooimayer, 1984).

Acknowledgements

It is a pleasure for us to thank Prof. E. Davoust whose suggestions as a referee helped in improving the paper.

References

Arenstorff, R. F. 1963, Amer. *J. Math*., **85**, 27.
Binney, J. J. 1978, *Mon. Not. R. astr. Soc*, **183**, 779.
Binney, J. J. 1981, *Mon. Not. R. astr. Soc*, **196**, 455.
Birkhoff, G D. 1927, *Dynamical Systems*, *Amer*. Math. Soc, New York.
Broucke, R. A. 1968, NASA-JPL Technical Report 32-1168.
Broucke, R. A. 1969, AIAA. Journal, **7**, 1003.
Colombo, G., Franklin, F. A., Munford, C. M. 1968, *Astr. J*., **73**, 111.
Contopoulos, G., Papayannopoulos, Th. 1980, *Astr. Astrophys*., **92**, 33.
Gelfand, I. M., Lindskii, V. B. 1955, *Usp. Mat. Nauk*, **10**, 3 (Amer. Math. Soc. Transl. **8**, 2.
Guillaume, P. 1969, *Astr. Astrophys*., **3**, 57.
Hadjidemetriou, J. D. 1975, *Celest. Mech*., **12**, 255.
Hadjidemetriou, J. D. 1979 in *Instabilities in Dynamical Systems*, Ed. V. G. Szebehely, D. Reidel, Dordrecht, p. 135.
Hadjidemetriou, J. D. 1982, *Celest. Mech*., **27**, 305.
Hadjidemetriou, J. D. 1985 in *Resonances in the Motion of Planets, Satellites and Asteroids*, Eds S. Ferraz-Mello & W. Sessin, Univ. de Sao Paulo, Brazil.
Hadjidemetriou, J. D., Ichtiaroglou, S. 1984, *Astr. Astrophys*., **131**, 20.
Henon. M. 1973, *Astr. Astrophys*., **28**, 415.
Krein, M. G. 1950, *Dokl. Akad. Nauk SSSR* N. S. **73**, 445.
Michalodimitrakis, M. 1979, *Astr.Astrophys*., **76**, 6.
Mulder, W. A., Hooimeyer, J. R. A. 1984, *Astr. Astrophys*., **134**, 158.
Schmidt, D. 1972, *SIAM J. Appl. Math*. **33**, No. 1.
Szebehely, V. 1967, *Theory of Orbits*, Academic Press, New York.
Zagouras, C, Markellos, V. V. 1977, *Astr. Astrophys*., **59**, 79.